Structural Engineering and Mechanics, *Vol. 74, No. 3 (2020) 425-434*
DOI: https://doi.org/10.12989/sem.2020.74.3.425

The effect of gravity and hydrostatic initial stress with variable thermal conductivity on a magneto-fiber-reinforced

Samia M. Said[a] and Mohamed I. A. Othman*

Department of Mathematics, Faculty of Science, Zagazig University,P.O. Box 44519, Zagazig, Egypt

(Received June 29, 2017, Revised October 5, 2017, Accepted November 27, 2019)

Abstract. The present paper is concerned at investigating the effect of hydrostatic initial stress, gravity and magnetic field in fiber-reinforced thermoelastic solid, with variable thermal conductivity. The formulation of the problem applied in the context of the three-phase-lag model, Green-Naghdi theory with energy dissipation, as well as coupled theory. The exact expressions of the considered variables by using state-space approaches are obtained. Comparisons are performed in the absence and presence of the magnetic field as well as gravity. Also, a comparison was made in the three theories in the absence and presence of variable thermal conductivity as well as hydrostatic initial stress. The study finds applications in composite engineering, geology, seismology, control system and acoustics, exploration of valuable materials beneath the earth's surface.

Keywords: Green-Naghdi theory III; three-phase-lag model; coupled theory; magnetic field; gravity; conductivity; hydrostatic initial stress

1. Introduction

The process of fiber-reinforcing has been developing continuously with advanced technology and the products are in use in various fields. Carbon fiber is ideal as a strengthening member in pipes for deepwater installations. Most concrete construction includes steel reinforcing, at least nominally. Fiber-reinforced materials are used for structures vulnerable to more or less violent vibrations during an earthquake and for similar disturbances. The study of wave propagation in a fiber-reinforced medium can justify the effectiveness of fiber-reinforcing in civil engineering and geophysics. Fiber-reinforced composites are widely used in engineering structures because of their superiority over the structural materials in applications requiring high strength and stiffness in lightweight components. A continuum model is used to explain the mechanical properties of such materials. A reinforced concrete member should be designed for all conditions of stresses that may occur and in accordance with principles of mechanics. The characteristic property of a reinforced concrete member is that its components, namely concrete and steel, act together as a single unit as long as they remain in the elastic condition (i.e., the two components are bonded together so that there can be no relative displacement between them). In the case of an elastic solid reinforced by a series of parallel fibers, it is usual to assume transverse isotropy. In the linear case, the associated constitutive relations, relating infinitesimal stress and strain components have five material constants. In the last three decades, the analysis of stress and deformation of fiber-reinforced composite materials has been an important research area of solid mechanics. Belfield *et al*. (1983) have introduced the idea of continuous self-reinforcement at every point of an elastic solid. Othman and Abbas (2011), Abbas *et al*. (2011), Abbas and Othman (2012) have done pioneer works on this subject. Fibers are assumed as an inherent material property rather than some form of inclusion in such models. One can find some work on transversely isotropic elasticity in the literature (Pipkin 1973, Othman and Said 2012).

During the last three decades, generalized theories involving a finite speed of heat transportation (hyperbolic heat transport equation) in elastic solids have been developed to remove this paradox. The first generalization is proposed by Lord and Shulman (1967) and is known as the extended thermoelasticity theory which involves one thermal relaxation time parameter (single-phase-lag model). The second generalization of the coupled thermoelasticity theory is developed by Green and Lindsay (1972), which involving two-thermal relaxation time is known as temperature rate-dependent thermoelasticity. The third generalization is known as low-temperature thermo-elasticity introduced by Hetnarski and Ignaczak (1999) called H–I theory. The fourth generalization is concerned with the thermoelasticity without energy dissipation and thermoelasticity with energy dissipation introduced by Green and Naghdi (1991, 1992, 1993) and provide sufficient basic modifications in the constitutive equations that permit treatment of a much wider class of heat flow problems, labeled as types I, II, III.

Another interesting field of recent study is in the field of magneto-thermoelasticity in which interacting effects of applied magnetic field on elastic and thermal deformations of a solid are studied. Such studies have applications in several areas, particularly in nuclear devices, biomedical engineering and geomagnetic investigations. Some of the

*Corresponding author, Ph.D.
E-mail: m_i_a_othman@yahoo.com
[a] Professor
E-mail: samia_said59@yahoo.com

ISSN: 1225-4568 (Print), 1598-6217 (Online)

works related to the interaction of the electromagnetic field, the thermal field, and the electric field may be available in kinds of literature by Marin and Craciun (2017), Marin and Nicaise (2016), Abbas (2014a,b), Abbas and Youssef (2013), Zenkour and Abbas (2014), Othman *et al*. (2019), Othman and Said (2014). A number of discussions relating wave propagation in rotating isotropic or transversely isotropic media were reported in literature by Roy Choudhuri (1984), Marin and Florea (2014), Marin, *et al*. (2017), Othman and Atwa (2014), Ahmad and Khan (2001), England and Rogers (1973), Othman and Said (2015), Othman and Abbas (2012), Said and Othman (2016).

In the present work, we shall formulate a magneto-fiber-reinforced thermoelastic medium with variable thermal conductivity under the effect of hydrostatic initial stress and gravity. State-space approach used to obtain the exact expressions for displacement components, force stresses and temperature. Distributions of the considered variables are given and represented graphically. Comparisons conducted between the considered variables as calculated from the 3PHL model, Green-Naghdi theory with dissipation (G-N III), and coupled theory in the presence and absence of magnetic field as well as variable thermal conductivity. A comparison is also made in the three theories in the presence and absence of gravity as well as hydrostatic initial stress.

2. Formulation of the problem and basic equations

We consider the problem of a fiber-reinforced thermoelastic half-space (x≥0). The medium is permeated into a uniform magnetic field with a constant intensity $\boldsymbol{H}=(0,H_0,0)$ which is parallel to the $y-$axis. We interested in a plane strain in the $xz-$ plane with displacement vector $\boldsymbol{u}=(u,0,w)$. The field equations and constitutive relations can be written as Belfield *et al*. (1983), Roy Choudhuri (1984), Montanaro (1999) and Othman *et al*. (2013) in the context of generalized thermoelasticity as follows:

The constitutive law of the theory of generalized thermo-elasticity is

$$\begin{aligned}\sigma_{ij} &= \lambda e_{kk}\delta_{ij} + 2\mu_T e_{ij} + \alpha(a_k a_m e_{km}\delta_{ij} + a_i a_j e_{kk}) \\ &+ 2(\mu_L - \mu_T)(a_i a_k e_{kj} + a_j a_k e_{ki}) \\ &+ \beta\, a_k a_m e_{km} a_i a_j - \gamma\hat{T}\,\delta_{ij} - P(\omega_{ij} + \delta_{ij}),\end{aligned} \tag{1}$$

$$\begin{aligned}\omega_{ij} &= \frac{1}{2}(u_{j,i} - u_{i,j}), \quad e_{ij} = \frac{1}{2}(u_{i,j} + u_{j,i}), \\ e_{kk} &= \frac{\partial u}{\partial x} + \frac{\partial w}{\partial z}, \; i,j = x,z,\end{aligned} \tag{2}$$

where, σ_{ij} are the components of stress, e_{ij} are the components of strain, e_{kk} is the dilatation, λ, μ are the elastic constants, $\gamma = (3\lambda + 2\mu)\ \alpha_t$ α_t is the thermal expansion coefficient, α, β, γ, (μ_L–μ_T) are the reinforcement parameters, P is the initial pressure, $\hat{T} = T - T_0$, where T is the temperature above the reference temperature T_0, $\delta_{ij,}$ is the Kronecker delta and $\boldsymbol{a} \equiv (a_1,a_2,a_3)$, $a_1^2 + a_2^2 + a_3^2 = 1$. We choose the fiber-direction as $\boldsymbol{a} \equiv (1,0,0)$. The heat conduction equation as Othman and Said (2014):

$$\begin{aligned}K^*\nabla^2 T + \tau_v^*\nabla^2\dot{T} + K\tau_T\nabla^2\ddot{T} &= [1+\tau_q\frac{\partial}{\partial t}+\frac{1}{2}\tau_q^2\frac{\partial^2}{\partial t^2}][\rho C_E n_0\ddot{T} \\ &+ \rho C_E n_1\dot{T} + \gamma T_0(n_2\frac{\partial}{\partial t}+n_3\tau_0\frac{\partial^2}{\partial t^2})e + \gamma T_0 n_4\dot{e}],\end{aligned} \tag{3}$$

where, K^* is the coefficient of thermal conductivity, K is the additional material constant, ρ is the mass density, C_E is the specific heat at constant strain, n_0,n_1,n_2,n_3,n_4 are integers, τ_0 thermal relaxation time τ_T and τ_q are the phase-lag of temperature gradient and the phase-lag of heat flux respectively. Also $\tau_v^* = K + \tau_v K^*$, where τ_v is the phase-lag of thermal displacement gradient.

Using Eqs. (1), then we have

$$\sigma_{xx} = A_{11}\frac{\partial u}{\partial x} + A_{12}\frac{\partial w}{\partial z} - \gamma\hat{T} - P, \tag{4}$$

$$\sigma_{zz} = A_{12}\frac{\partial u}{\partial x} + A_{22}\frac{\partial w}{\partial z} - \gamma\hat{T} - P, \tag{5}$$

$$\sigma_{xz} = S_1\frac{\partial u}{\partial z} + S_2\frac{\partial w}{\partial x}, \tag{6}$$

$$\sigma_{zx} = S_2\frac{\partial u}{\partial z} + S_1\frac{\partial w}{\partial x}. \tag{7}$$

Where

$$A_{11} = \lambda + 2(\mu_T + \alpha) + 4(\mu_{L-}\mu_T) + \beta,$$

$$A_{12} = \lambda + \alpha,\ A_{22} = \lambda + 2\mu_T,$$

$$S_1 = \mu_L + \frac{P}{2},\quad S_2 = \mu_L - \frac{P}{2}.$$

The equation of motion:

$$\rho\ddot{u}_i = \sigma_{ji,j} + \mu_0\,(\boldsymbol{J}\times\boldsymbol{H})_i + F_i. \tag{8}$$

Where

$$F_1 = \rho g\frac{\partial w}{\partial x},\quad F_2 = 0,\quad F_3 = -\rho g\frac{\partial u}{\partial x}.$$

The variation of the magnetic and electric fields are perfectly conducting slowly moving medium and are given by Maxwell's equation as Othman and Said (2015)

$$\boldsymbol{J} = \nabla\times\boldsymbol{h} - \varepsilon_0\frac{\partial\boldsymbol{E}}{\partial t},\ \nabla\times\boldsymbol{E} = -\mu_0\frac{\partial\boldsymbol{h}}{\partial t},\ \boldsymbol{E} = -\mu_0(\dot{\boldsymbol{u}}\times\boldsymbol{H}),\ \nabla.\boldsymbol{h} = 0. \tag{9}$$

Where μ_0 is the magnetic permeability, ε_0 is electric permeability, $\boldsymbol{J}$ is the current density vector and $\dot{\boldsymbol{u}}$ is the particle velocity of the medium and the small effect of temperature gradient on $\boldsymbol{J}$ is also ignored. Expressing the components of the vector $\boldsymbol{J} = (J_1,J_2,J_3)$ in terms of displacement by eliminating the quantities $\boldsymbol{h}$ and $\boldsymbol{E}$ from Eq. (9), thus yields

$$\begin{aligned}G_1 &= -\mu_0 H_0\frac{\partial h}{\partial x} - \varepsilon_0\mu_0^2 H_0^2\frac{\partial^2 u}{\partial t^2},\qquad G_2 = 0, \\ G_3 &= -\mu_0 H_0\frac{\partial h}{\partial z} - \varepsilon_0\mu_0^2 H_0^2\frac{\partial^2 w}{\partial t^2}.\end{aligned} \tag{10}$$

Where

$$\boldsymbol{G}_{\mathrm{i}} = \mu_0\ (\boldsymbol{J} \times \boldsymbol{H}\ )_{\mathrm{i}}$$

Introducing Eqs. (4) - (7) and (10) in Eqs. (8), thus we have

$$\rho \frac{\partial^2 u}{\partial t^2} = A_{11} \frac{\partial^2 u}{\partial x^2} + B_1 \frac{\partial^2 w}{\partial x \partial z} + S_2 \frac{\partial^2 u}{\partial z^2} - \gamma \frac{\partial \hat{T}}{\partial x} + \rho g \frac{\partial w}{\partial x} - \mu_0 H_0 \frac{\partial h}{\partial x} - \varepsilon_0 \mu_0^2 H_0^2 \frac{\partial^2 u}{\partial t^2}, \tag{11}$$

$$\rho \frac{\partial^2 w}{\partial t^2} = S_2 \frac{\partial^2 w}{\partial x^2} + B_1 \frac{\partial^2 u}{\partial x \partial z} + A_{22} \frac{\partial^2 w}{\partial z^2} - \gamma \frac{\partial \hat{T}}{\partial z} - \rho g \frac{\partial u}{\partial x} - \mu_0 H_0 \frac{\partial h}{\partial z} - \varepsilon_0 \mu_0^2 H_0^2 \frac{\partial^2 w}{\partial t^2}, \tag{12}$$

where,

$B_1 = A_{12} + S_1.$

3. Variable thermal conductivity

Generally, the assumption that the solid body is thermo-sensitivity (the thermal properties of the material vary with temperature) leads to a nonlinear heat conduction problem. The exact solution of such a problem can be found by assuming the material to be (simply nonlinear) meaning that the thermal conductivity K^* and C_E specific heat depend on the temperature. The thermal conductivity K^* is assumed to vary linearly with temperature according to (Noda 1986)

$$K^* = K^*(\theta) = K_0(1 + K_1\theta). \tag{13}$$

Where K_0 is the thermal conductivity at ambient temperature T_0 and K_1 is the slope of the thermal conductivity-temperature curve divided by the intercept K_0. Now, we will consider the Kirchhoff transformation (Noda 1986)

$$\psi = \frac{1}{K_0} \int_0^{\theta} K^*(\theta')\, d\theta'. \tag{14}$$

where ψ is a new function expressing the heat conduction. The above equation with the aid of Eq. (13) gives

$$\psi = \theta\left(1 + \frac{K_1}{2}\theta\right). \tag{15}$$

From Eqs. (13) and (15), it follows that

$$\frac{\partial \theta}{\partial x_i} = \frac{1}{(1 + K_1\theta)} \frac{\partial \psi}{\partial x_i} = \frac{\partial \psi}{\partial x_i}[1 - K_1\theta + (K_1\theta)^2 - (K_1\theta)^3 + \ldots], \tag{16}$$

$$\frac{\partial \theta}{\partial t} = \frac{1}{(1 + K_1\theta)} \frac{\partial \psi}{\partial t} = \frac{\partial \psi}{\partial t}[1 - K_1\theta + (K_1\theta)^2 - (K_1\theta)^3 + \ldots]. \tag{17}$$

For linearity, since $\theta = T - T_0$, such that $|\theta / T_0| \le 1$, then the above equation will be reduced to

$$\frac{\partial \theta}{\partial x_i} = \frac{\partial \psi}{\partial x_i}, \qquad \frac{\partial \theta}{\partial t} = \frac{\partial \psi}{\partial t}. \tag{18}$$

From Eqs. (15) and (18) in Eqs. (11), (12) and (3), thus we have

$$\rho \frac{\partial^2 u}{\partial t^2} = A_{11} \frac{\partial^2 u}{\partial x^2} + B_1 \frac{\partial^2 w}{\partial x \partial z} + S_2 \frac{\partial^2 u}{\partial z^2} - \gamma \frac{\partial \psi}{\partial x} + \rho g \frac{\partial w}{\partial x} - \mu_0 H_0 \frac{\partial h}{\partial x} - \varepsilon_0 \mu_0^2 H_0^2 \frac{\partial^2 u}{\partial t^2}, \tag{19}$$

$$\rho \frac{\partial^2 w}{\partial t^2} = S_2 \frac{\partial^2 w}{\partial x^2} + B_1 \frac{\partial^2 u}{\partial x \partial z} + A_{22} \frac{\partial^2 w}{\partial z^2} - \gamma \frac{\partial \psi}{\partial z} - \rho g \frac{\partial u}{\partial x} - \mu_0 H_0 \frac{\partial h}{\partial z} - \varepsilon_0 \mu_0^2 H_0^2 \frac{\partial^2 w}{\partial t^2}, \tag{20}$$

$$K_0 \nabla^2 \psi + (K + \tau_\upsilon K_0)\nabla^2 \dot{\psi} + K \tau_T \nabla^2 \ddot{\psi} = [1 + \tau_q \frac{\partial}{\partial t} + \frac{1}{2}\tau_q^2 \frac{\partial^2}{\partial t^2}][\rho C_E n_0 \ddot{\psi} + \rho C_E n_1 \dot{\psi} + \gamma T_0 (n_2 \frac{\partial}{\partial t} + n_3 \tau_0 \frac{\partial^2}{\partial t^2}) e + \gamma T_0 n_4 \ddot{e}]. \tag{21}$$

Introducing the following non-dimension quantities in the above equation (dropping the primes for convenience):

$$(x', z', u', w') = c_1\eta(x, z, u, w),\ g' = \frac{g}{c_1^3 \eta},\ \psi' = \frac{\gamma\ \psi}{A_{11}},\ h' = \frac{h}{H_0},\ P' = P, \tag{22}$$

$$(t', \tau_q', \tau_\nu', \tau_T', \tau_0') = c_1^2 \eta\ (t, \tau_q, \tau_\nu, \tau_T, \tau_0),\quad \sigma_{ij}' = \frac{\sigma_{ij}}{\mu_T},\quad i, j = 1, 2,$$

where

$$\eta = \frac{\rho C_E}{K_0}, \qquad c_1^2 = \frac{A_{11}}{\rho}.$$

Thus we get,

$$C_0 \frac{\partial^2 u}{\partial t^2} = m_0 \frac{\partial^2 u}{\partial x^2} + m_1 \frac{\partial^2 w}{\partial x \partial z} + m_2 \frac{\partial^2 u}{\partial z^2} + g \frac{\partial w}{\partial x} - \frac{\partial \psi}{\partial x}, \tag{23}$$

$$C_0 \frac{\partial^2 w}{\partial t^2} = m_2 \frac{\partial^2 w}{\partial x^2} + m_1 \frac{\partial^2 u}{\partial x \partial z} + m_3 \frac{\partial^2 w}{\partial z^2} - \frac{\partial \psi}{\partial z} - g \frac{\partial u}{\partial x}, \tag{24}$$

$$C_K \psi_{,ii} + C_\nu \dot{\psi}_{,ii} + C_T \ddot{\psi}_{,ii} = [1 + \tau_q \frac{\partial}{\partial t} + \frac{1}{2}\tau_q^2 \frac{\partial^2}{\partial t^2}][n_0 \ddot{\psi} + n_1 \varepsilon_1 \dot{\psi} + \varepsilon_2 (n_2 \frac{\partial}{\partial t} + n_3 \tau_0 \frac{\partial^2}{\partial t^2}) e + \varepsilon_3 n_4 \ddot{e}], \tag{25}$$

where

$$C_0 = 1 + \frac{\varepsilon_0 \mu_0^2 H_0^2}{\rho},\quad m_0 = 1 + \frac{\mu_0 H_0^3}{A_{11}},\quad m_1 = \frac{B_1 + \mu_0 H_0^3}{A_{11}},\quad m_2 = \frac{S_2}{A_{11}},$$
$$m_3 = \frac{A_{22} + \mu_0 H_0^3}{A_{11}},\quad C_K = \frac{K_0}{\rho C_E c_1^2},\ C_\nu = \frac{\eta c_1^2 K + K_0 \tau_\nu}{\rho C_E c_1^2},\quad C_T = \frac{\eta K \tau_T}{\rho C_E},$$
$$\varepsilon_1 = \frac{1}{c_1^2 \eta},\qquad \varepsilon_2 = \frac{\gamma^2 T_0}{\rho C_E A_{11} c_1^2 \eta},\qquad \varepsilon_3 = \frac{\gamma^2 T_0}{\rho C_E A_{11}}.$$

For harmonic solutions of the Eqs. (23)-(25), we choose

$$[u, w, e, \psi, \sigma_{ij}](x, z, t) = [\bar{u}, \bar{w}, \bar{e}, \bar{\psi}, \sigma_{ij}](z) \exp(ct + \mathrm{i}bx). \tag{26}$$

Where $\bar{u}(z)$, etc. is the amplitude of the function $u(x, z, t)$ etc., i is the imaginary unit, c (complex) is the time constant and b is the wave number in the $x-$ direction.

Introducing Eq. (26) in Eqs. (23) - (25), we get

$$\mathrm{D}^2 \bar{u} = C_1 \bar{u} + C_2 \bar{w} + C_3 \bar{\psi} + C_4 \mathrm{D}\bar{w}, \tag{27}$$

$$\mathrm{D}^2 \bar{w} = C_5 \bar{u} + C_6 \bar{w} + C_7 \mathrm{D}\bar{u} + C_8 \mathrm{D}\bar{\psi}, \tag{28}$$

$$\mathrm{D}^2\bar{\psi} = C_{14}\bar{u} + C_{15}\bar{\psi} + C_{16}\mathrm{D}\bar{w}, \tag{29}$$

where

$$C_1 = \frac{C_0c^2 + m_0b^2}{m_2},\quad C_2 = \frac{-\mathrm{i}bg}{m_2},\quad C_3 = \frac{\mathrm{i}b}{m_2},\quad C_4 = \frac{-\mathrm{i}bm_1}{m_2},\quad C_5 = \frac{\mathrm{i}bg}{m_3},$$

$$C_6 = \frac{C_0c^2 + m_2b^2}{m_3},\ C_7 = \frac{-\mathrm{i}bm_1}{m_3},\ C_8 = \frac{1}{m_3},\ C_9 = C_K + C_vc + C_Tc^2,\ C_{10} = b^2C_9,$$

$$C_{11} = (1 + \tau_q c + \frac{1}{2}\tau_q^2 c^2)(n_0c^2 + n_1\varepsilon_1 c),$$

$$C_{12} = (1 + \tau_q c + \frac{1}{2}\tau_q^2 c^2)(n_2\varepsilon_2 c + n_3\varepsilon_2\tau_0 c^2 + n_4\varepsilon_3 c^2),\quad C_{13} = \mathrm{i}b\,C_{12},\quad C_{14} = \frac{C_{13}}{C_9},$$

$$C_{15} = \frac{C_{10} + C_{11}}{C_9},\quad C_{16} = \frac{C_{12}}{C_9},\quad \mathrm{D} = \frac{\mathrm{d}}{\mathrm{d}z}.$$

The system of Eqs. (27)-(29) can be written in a vector-matrix differential equation in the following way as (Othman and Said 2015, Noda 1986, Zorammuana and Singh 2015)

$$\mathrm{D}V(z) = A(c,b)V(z). \tag{30}$$

Where

$V(x) = [\bar{u}, \bar{w}, \bar{\psi}, \mathrm{D}\bar{u}, \mathrm{D}\bar{w}, \mathrm{D}\bar{\psi}]^{\mathrm{T}}$,

$$A = \begin{bmatrix} 0 & 0 & 0 & 1 & 0 & 0 \\ 0 & 0 & 0 & 0 & 1 & 0 \\ 0 & 0 & 0 & 0 & 0 & 1 \\ C_1 & C_2 & C_3 & 0 & C_4 & 0 \\ C_5 & C_6 & 0 & C_7 & 0 & C_8 \\ C_{14} & 0 & C_{15} & 0 & C_{16} & 0 \end{bmatrix}. \tag{31}$$

4. Solution of the vector-matrix differential equation

Following the solution methodology through the eigen value approach (Othman and Said 2015), we now proceed to solve the vector-matrix differential equation (30). The characteristic equation of a matrix A is (by using the Matlab program)

$$E^6 - F_1\,\mathrm{E}^4 + F_2\,\mathrm{E}^2 - F_3 = 0, \tag{32}$$

where

$$F_1 = C_8C_{16} + C_4C_7 + C_{15} + C_{16} + C_1,$$
$$F_2 = C_4C_7C_{15} + C_6C_{15} - C_3C_7C_{16} - C_4C_8C_{14} + C_1C_8C_{16} + C_1C_{15} - C_3C_{14} + C_1C_6 - C_2C_5,$$
$$F_3 = C_1C_6C_{15} - C_2C_5C_{15} - C_3C_{14}C_6.$$

Let E_1^2, E_2^2, E_3^2 be the roots of the characteristic Eq. (32) with positive real parts. Then all the six roots of the above characteristic equation, which are also the eigen values of the matrix A are of the form $\mathrm{E} = \pm\mathrm{E}_1, \pm\mathrm{E}_2, \pm\mathrm{E}_3$.

Suppose $\chi = [x_1, x_2, x_3, x_4, x_5, x_6]^T$ be a right eigenvector corresponding to the eigen value E of the matrix A. Then, after simple manipulations, we get

$$x_1 = E^2(C_4C_8 + C_3) + C_2C_8E - C_6C_3,$$
$$x_2 = C_8E^3 + E(C_3C_7 - C_1C_8) + C_3C_5, \tag{33}$$
$$x_3 = C_{14}C_6 - C_5C_{16}E - E^2(C_{14} + C_7C_{16}),$$
$$x_4 = E\,x_1,\quad x_5 = E\,x_2,\quad x_6 = E\,x_3.$$

From (33), we can easily calculate the eigenvector $\chi_j, (j = 1, 2, 3)$ corresponding to the eigenvalue $\pm E_j, (j = 1, 2, 3)$. For our further reference, we shall use the following notations

$\chi_1 = [\chi]_{E=E_1}$, $\chi_2 = [\chi]_{E=-E_1}$, $\chi_3 = [\chi]_{E=E_2}$, $\chi_4 = [\chi]_{E=-E_2}$, $\chi_5 = [\chi]_{E=E_3}$ $\chi_6 = [\chi]_{E=-E_3}$.

Solution of Eq. (30) which is bound as $z \to \infty$, is given by

$$\bar{u}(z) = \sum_{j=1}^{3} x_{1j}\,R_j\,\exp(-E_jz), \tag{34}$$

$$\bar{w}(z) = \sum_{j=1}^{3} x_{2j}\,R_j\,\exp(-E_jz), \tag{35}$$

$$\bar{\psi}(z) = \sum_{j=1}^{3} x_{3j}\,R_j\,\exp(-E_jz), \tag{36}$$

where R_j are parameters,

$x_{1j} = [x_1]_{E=-E_j}$, $x_{2j} = [x_2]_{E=-E_j}$, $x_{3j} = [x_3]_{E=-E_j}$, $j = 1, 2, 3.$

Introduce Eqs. (15), (22), (26) and (34) - (36) in Eqs. (5)-(6), we get

$$\bar{\sigma}_{zz} = \sum_{j=1}^{3} x_{4j}\,R_j\,\exp(-E_jz) - \frac{P^*}{\mu_{\mathrm{T}}}, \tag{37}$$

$$\bar{\sigma}_{xz} = \sum_{j=1}^{3} x_{5j}\,R_j\,\exp(-E_jz), \tag{38}$$

where

$$x_{4j} = \frac{1}{\mu_T}[\mathrm{i}bA_{12}x_{1j} - A_{22}E_j\,x_{2j} - A_{11}x_{3j}],$$
$$x_{5j} = \frac{1}{\mu_T}[-S_1E_jx_{1j} + \mathrm{i}bS_2\,x_{2j}],\quad P^* = P\exp(-ct - \mathrm{i}bx).$$

5. Application

In this section we determine the parameters R_j (j=1,2,3) In the physical problem, we should suppress the positive exponential that unbounded at infinity. The constants R_j (j=1,2,3) have chosen such that the boundary conditions on the surface at $z = 0$ are as follows:

$$\sigma_{zz} = -R_pf^*\exp(ct + \mathrm{i}b\,x) - \frac{P}{\mu_T},\quad \sigma_{xz} = 0,\qquad \psi = \psi_1. \tag{39}$$

Where f^* is constant, Rp is the magnitude of hydrostatic initial stress and $\psi_1 = p_2 + \frac{1}{2}p_2^2K_1$.

Using the expressions of the variables considered into the above boundary conditions (Eqs. (39)), we can obtain the following equations satisfied with the parameters:

$$\sum_{j=1}^{3} x_{3j} R_j = \psi_0, \quad \sum_{j=1}^{3} x_{4j} R_j = -R_P f^*, \quad \sum_{j=1}^{3} x_{5j} R_j = 0. \quad (40)$$

Where $\psi_0 = \psi_1 \exp(-ct - ibx)$. Invoking Eqs. (40), we obtain a system of three equations. After applying the inverse of the matrix method, we have the values of the three constants R_j (j=1,2,3)

Hence, we obtain expressions for the displacements, temperature distribution, and other physical quantities.

$$\begin{pmatrix} R_1 \\ R_2 \\ R_3 \end{pmatrix} = \begin{pmatrix} x_{31} & x_{32} & x_{33} \\ x_{41} & x_{42} & x_{43} \\ x_{51} & x_{52} & x_{53} \end{pmatrix}^{-1} \begin{pmatrix} \psi_0 \\ -R_P f^* \\ 0 \end{pmatrix}. \quad (41)$$

After obtaining ψ, the temperature increment θ can be obtained by solving Eq. (15) to give

$$\Theta = \frac{-1 + \sqrt{1 + 2K_1\psi}}{K_1}. \quad (42)$$

6. Particular cases and special cases of thermo-elastic theory

i. A magneto-fiber-reinforced generalized thermoelastic medium under effect of gravity and hydrostatic initial stress without temperature-dependent thermal conductivity from above equations with K_1=0.

ii. A fiber-reinforced generalized thermoelastic medium under effect of gravity and hydrostatic initial stress with temperature-dependent thermal conductivity from above equations with H_1=0.

iii. A magneto-fiber-reinforced generalized thermoelastic medium under the effect of hydrostatic initial stress with temperature-dependent thermal conductivity from the above equations with g=0.

iv. A magneto-fiber-reinforced generalized thermoelastic medium under the effect of gravity with temperature-dependent thermal conductivity from above equations with R_p=0.

v. Equations of the 3PHL model when n0=n4=1 $n_0 = n_4 = 1, \quad n_1 = n_2 = n_3 = \tau_0 = 0, \quad K, \tau_T, \tau_q, \tau_v > 0$ and the solutions are always (exponentially) stable if $\frac{2K\tau_T}{\tau_q} > \tau_v^* > K^*\tau_q$ as in Quintanilla and Racke (2008).

vi. Equations of the G-N II theory when,
$n_0 = n_4 = 1, \; n_1 = n_2 = n_3 = 0, \quad K = \tau_T = \tau_q = \tau_v = \tau_0 = 0.$

vii. Equations of the G-N III theory when,
$n_0 = n_4 = 1, \; n_1 = n_2 = n_3 = 0, \quad \tau_T = \tau_q = \tau_v = \tau_0 = 0.$

viii. Equations of the L-S theory when,
$n_4 = 0, \; n_0, \tau_0 > 0, \quad n_1 = n_2 = n_3 = 1, \quad K = \tau_T = \tau_q = \tau_v = 0.$

ix. Equations of the CD theory when,
$n_4 = n_0 = n_3 = 0, \; n_1 = n_2 = 1, \quad K = \tau_T = \tau_q = \tau_v = \tau_0 = 0.$

7. Numerical calculation and discussion

In order to illustrate the theoretical results obtained in the preceding section, and to compare these in the context of the above theories, we now present some numerical results for the physical constants as Othman and Said (2014):

$$\lambda = 1.76 \text{x} 10^9 \text{ N.m}^{-2}, \; \mu = 3.78 \text{x} 10^{10} \text{ N.m}^{-2}, \; \mu_0 = 1.7,$$

$$\rho = 7800 \text{ kg.m}^{-3}, \; C_E = 383..3 \text{ J.kg}^{-1}.\text{K}^{-1}, \; \varepsilon_0 = 0.3,$$

$$\mu_T = 1.89 \text{x} 10^9 \text{ N.m}^{-2}, \; \mu_L = 2.45 \text{x} 10^9 \text{ N.m}^{-2}, \; H_0 = 180,$$

$$\tau_q = 0.9\text{s}, \; \tau_v = 0.6\text{s}, \; \alpha_t = 1.78 \text{ x} 10^{-4} \text{ K}^{-1}, g = 9.8 \text{ m.s}^{-2},$$

$$K = 200 \text{w.m}^{-1}.\text{K}^{-1}, \quad \alpha = -1.28 \text{x} 10^9 \text{ N.m}^{-2}, \; \beta = 0.32 \text{x} 10^9 \text{ N.m}^{-2},$$

$$c = \xi_0 + i\,\xi, \quad \xi_0 = 0.3, \quad \xi = -0.6, \quad b = 0.4, \quad \tau_T = 0.7\text{s},$$

$$P = 1.45 \text{ x} 10^5 \text{ N.m}^{-2}, \quad R_P = 1.9 \text{N.m}^{-2}, \; T_0 = 293\text{K},$$

$$f^* = 0.9, \quad p_2 = 0.3, \quad K_1 = -10 \text{ T}^{-1}.$$

The computations carried out for a value of time t= 0.05s. The horizontal displacement component u, the thermal temperature θ, and the stress components σ_{zz}, σ_{xz} with distance z for the value of x, namely $x = 0.5\text{m}$, substituted in performing the computations. The results are shown in figs. 1–16. The graphs show six curves predicted by three different theories of thermoelasticity. In these figures, the solid lines represent the solution in the 3PHL model, the dashed lines represent the solution derived using the G-N III theory and the dotted line represents the solution derived using the CD theory.

Figs. 1-4 show comparisons between the horizontal displacement components u, the thermal temperature θ, and the stress components σ_{zz}, σ_{xz} with temperature-dependent and temperature-independent thermal conductivity. Fig. 1 depicts that the distribution of the horizontal displacement u begins from negative values. In the context of the three theories with temperature-dependent thermal conductivity, u starts with increasing to the maximum value, then decreases, and again increases. However, in the context of the three theories with temperature-independent thermal conductivity u starts with decreasing, and again increases. The values of u increase with temperature-dependent thermal conductivity in the first, then decrease and last become constant. It is clear from fig. 2 that the thermal temperature θ begins from negative values with temperature-dependent thermal conductivity, but it begins from positive values with temperature-independent thermal conductivity and satisfies the boundary condition at z=0, In the context of the three theories with temperature-dependent thermal conductivity, θ increases to maximum values, then decreases, and last become constant. However, in the context of the three theories with temperature-independent thermal conductivity, θ decreases, then increases and last becomes constant. The values of θ start decrease, then increasing with temperature-dependent thermal conductivity and last become constant. Fig. 3 displays that the distribution of the stress component σ_{zz} begins from

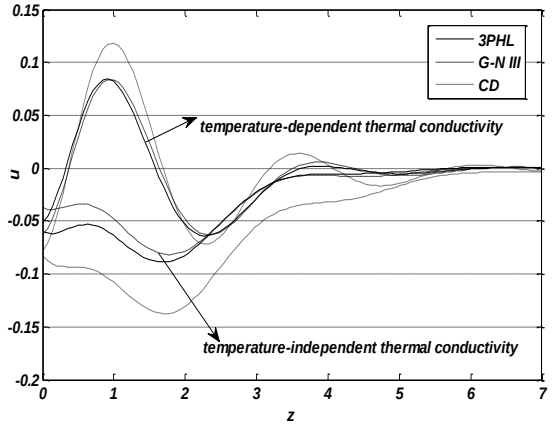

Fig. 1 Horizontal displacement distribution u with and without temperature thermal conductivity

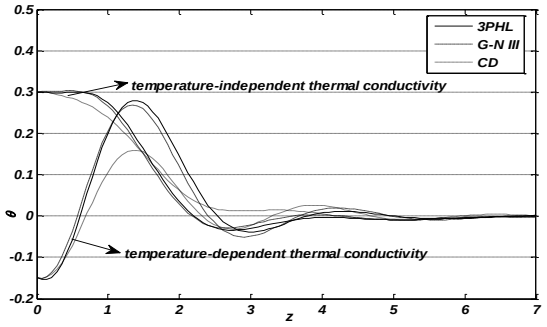

Fig. 2 Thermal temperature distribution θ with and without temperature thermal conductivity

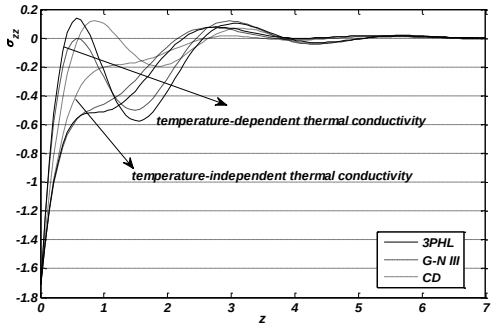

Fig. 3 Distribution of stress component σ_{zz} with and without temperature thermal conductivity

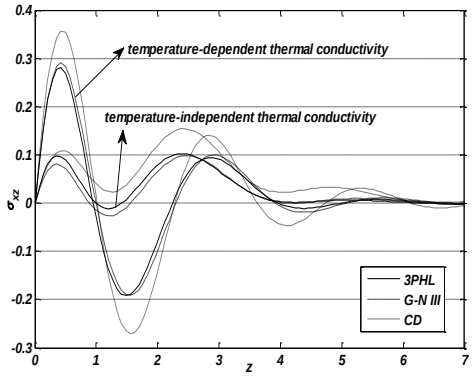

Fig. 4 Distribution of stress component σ_{xz} with and without temperature thermal conductivity

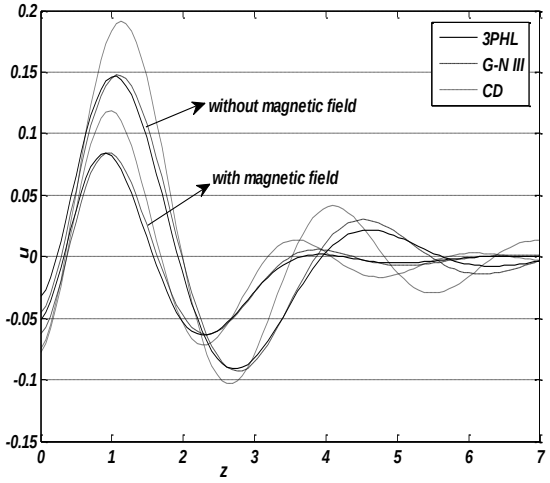

Fig. 5 Horizontal displacement distribution u in the absence and presence of magnetic field

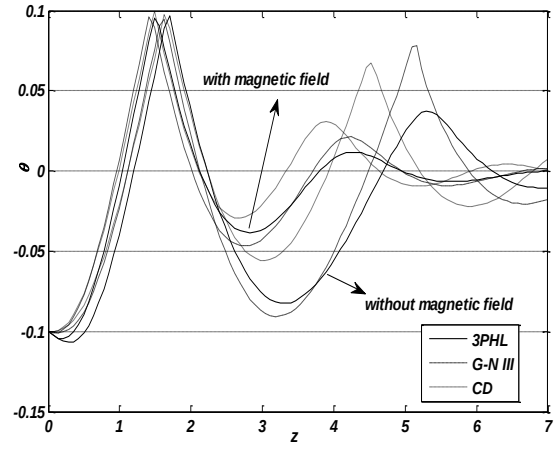

Fig. 6 Thermal temperature distribution θ in the absence and presence of magnetic field

negative values and satisfies the boundary condition at z=0. In the context of the three theories with temperature-dependent thermal conductivity, σ_{zz} starts with increasing to maximum values, then decreases, and moves in wave propagation. However, the context of the three theories with temperature-independent thermal conductivity, σ_{zz} starts with increasing, then decreases, and becomes constant. The temperature-dependent thermal conductivity increases the values of σ_{zz} and then decreases theirs. Fig. 4 shows the distribution of the stress component σ_{xz} and demonstrates that it reaches a zero value and satisfies the boundary condition at z=0. In the context of the three theories, σ_{xz} starts with increasing, and then decreases and moves in wave propagation. The values of σ_{xz} increase, then decrease and again increases with temperature-dependent thermal conductivity. Figs. 1-4 demonstrate that temperature-dependent thermal conductivity has a significant role in all the physical quantities.

Figs. 5–8 show comparisons between the horizontal displacement component u, the thermal temperature θ, and the stress components σ_{zz}, σ_{xz} with and without the magnetic

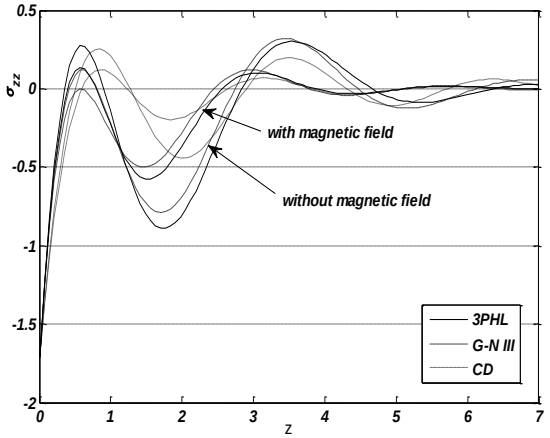

Fig. 7 Distribution of stress component σ_{zz} in the absence and presence of magnetic field

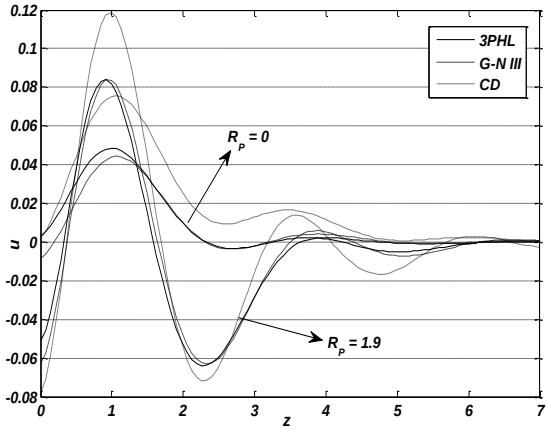

Fig. 9 Horizontal displacement distribution u in the absence and presence of hydrostatic initial stress

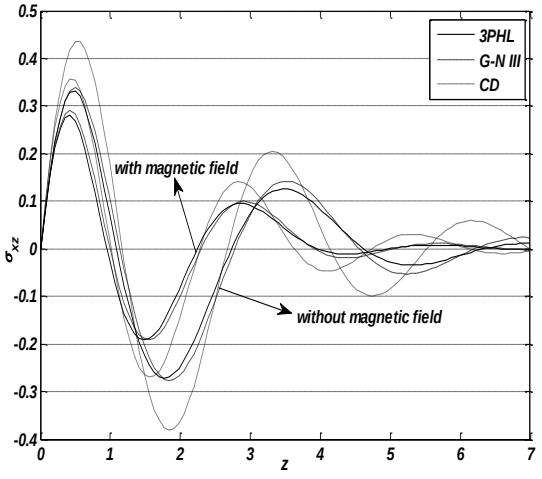

Fig. 8 Distribution of stress component σ_{xz} in the absence and presence of magnetic field

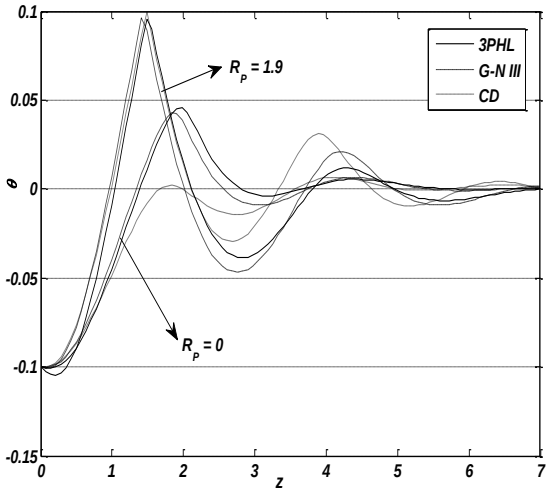

Fig. 10 Thermal temperature distribution θ in the absence and presence of hydrostatic initial stress

field. Fig. 5 depicts the distribution of the horizontal displacement u. In the context of the three theories without the effect of the magnetic field, u starts with increasing to the maximum value, then decreases, and moves in wave propagation. The values of u decrease with the effect of the magnetic field in the first, then increase, again decrease, and last increase. It is clear from fig. 6 that the thermal temperature θ begins from negative values and satisfies the boundary condition at z=0 In the context of the three theories without the effect of the magnetic field, θ increases to maximum values, then decreases, again increases, and last decreases. The values of θ decrease, then increase, again decrease, and last increase with the effect of the magnetic field. Fig. 7 displays that the distribution of the stress component σ_{zz} begins from negative values and satisfies the boundary condition at z=0. In the context of the three theories without the effect of the magnetic field, σ_{zz} starts with increasing to maximum values, then decreases, and moves in wave propagation. The magnetic field decreases the values of σ_{zz} then increase, again decrease, and last increase. Fig. 8 shows the distribution of the stress component σ_{xz} and demonstrates that it reaches a zero value and satisfies the boundary condition at z=0. In the context of the three theories, σ_{xz} starts with increasing to maximum values, then decreases and moves in wave propagation. The values of σ_{xz} decrease then increase, then decrease and again increases with the effect of the magnetic field. Figs. 5-8 demonstrate that the magnetic field has a significant role in all the physical quantities.

Figs. 9-12 show comparisons between the horizontal displacement component u, the thermal temperature θ, and the stress components σ_{zz}, σ_{xz} with and without the effect of hydrostatic initial stress. Fig. 9 depicts the distribution of the horizontal displacement u. In the context of the three theories without the effect of hydrostatic initial stress, u starts with increasing to the maximum value, then decreases. The values of u decrease with the effect of hydrostatic initial stress in the first, then increase and again decrease. It is clear from fig. 10 that the thermal temperature θ begins from negative values and satisfies the boundary condition at

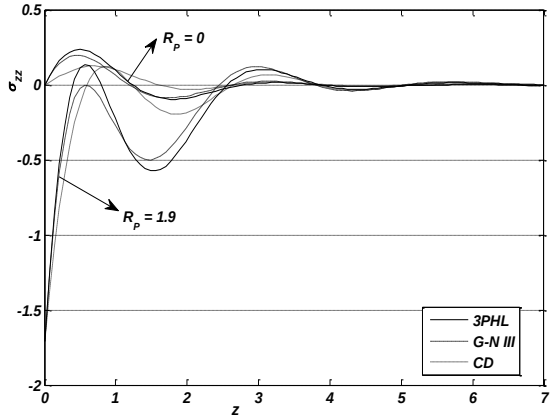

Fig. 11 Distribution of stress component σ_{zz} in the absence and presence of hydrostatic initial stress

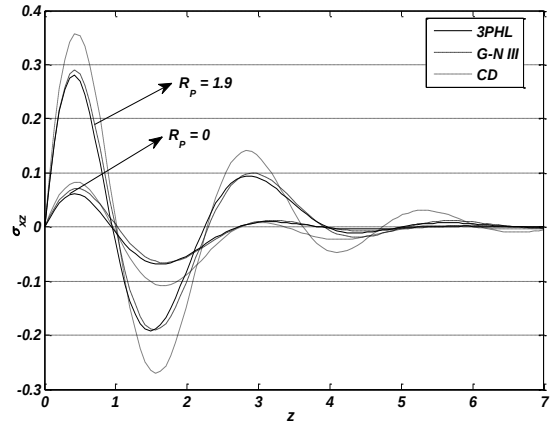

Fig. 12 Distribution of stress component σ_{zz} in the absence and presence of hydrostatic initial stress

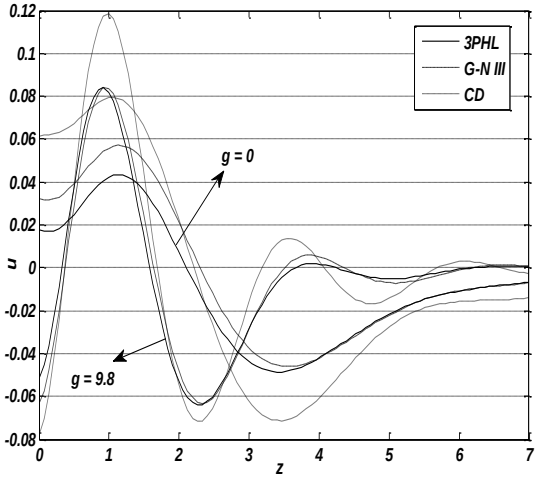

Fig. 13 Horizontal displacement distribution u in the absence and presence of gravity

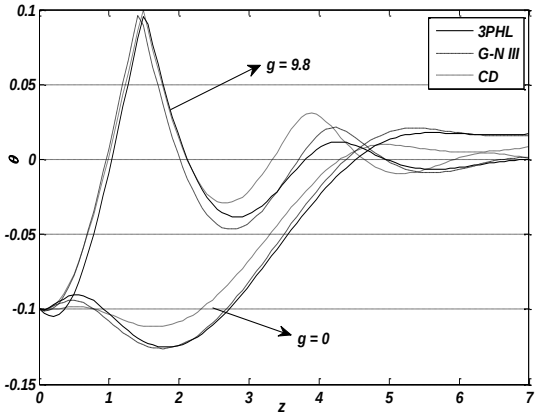

Fig. 14 Thermal temperature distribution θ in the absence and presence of gravity

z=0. In the context of the three theories without the effect of hydrostatic initial stress, θ increases to maximum values, then decreases, and last becomes constant. The values of θ increase, then decrease and again increase with the effect of hydrostatic initial stress. Fig. 11 displays that the distribution of the stress component σ_{zz} begins from negative values and satisfies the boundary condition at z=0. In the context of the three theories without the effect of hydrostatic initial stress, σ_{zz} starts with increasing to maximum values, then decreases, and moves in wave propagation. The hydrostatic initial stress decrease values of $\sigma_{zz,}$ then increase. Fig. 12 shows the distribution of the stress component σ_{xz} and demonstrates that it reaches a zero value and satisfies the boundary condition at z=0. In the context of the three theories, σ_{xz} starts with increasing to the maximum values, then decreases and moves in wave propagation. The values of σ_{xz} increase, then decrease and then increase with the effect of hydrostatic initial stress. Figs. 9-12 demonstrate that the hydrostatic initial stress has a significant role in all the physical quantities.

Figs. 13–16 show comparisons between the horizontal displacement component u, the thermal temperature θ, and the stress components $\sigma_{zz,}$ σ_{xz} with and without the effect of the gravity field. Fig. 13 depicts the distribution of the horizontal displacement u, In the context of the three theories without the effect of the gravity field, u starts with increasing to the maximum value, then decreases and again increases. The values of u decrease with the effect of the gravity in the first, then increase, again decrease and last increase. It is clear from fig. 14 that the thermal temperature θ begins from negative values and satisfies the boundary condition at z=0. In the context of the three theories without the effect of the gravity, θ decreases and then increases. The values of θ increase then decrease with the effect of the gravity field. Fig. 15 displays that the distribution of the stress component σ_{zz} begins from negative values and satisfies the boundary condition at z=0 In the context of the three theories without the effect of the gravity field, σ_{zz} starts with increasing to maximum values, then decreases, and moves in wave propagation. The gravity decreases the values of σ_{zz} and then increase. Fig. 16 shows the distribution of the stress component σ_{xz} and demonstrates that it reaches a zero value and satisfies the boundary condition at z=0. In the context of the three theories without

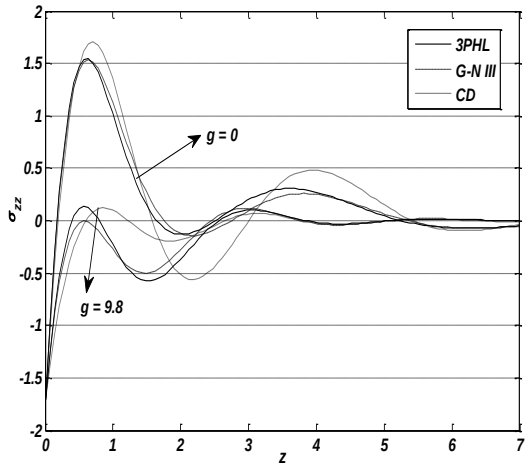

Fig. 15 Distribution of stress component σ_{zz} in the absence and presence of gravity

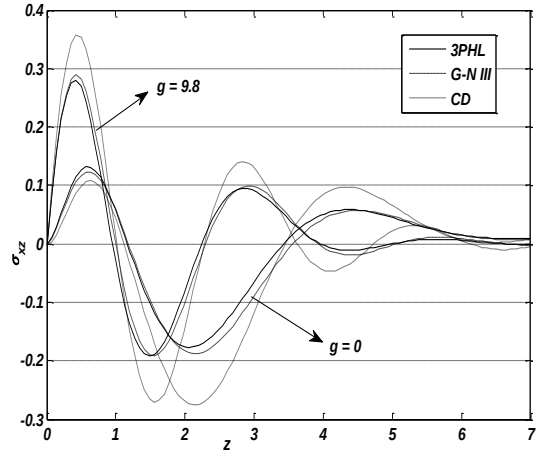

Fig. 16 Distribution of stress component σ_{zz} in the absence and presence of gravity

the effect of gravity, σ_{xz} starts with increasing to the maximum values, then decreases to minimum value and moves in wave propagation. The values of σ_{xz} increase, then decreasing, again increase and last decrease with the effect of the gravity. Figs. 13-16 demonstrate that the gravity field has a significant role in all the physical quantities.

8. Conclusion

In the present study, the state-space approach is used to study the effect of the hydrostatic initial stress, temperature-dependent thermal conductivity, magnetic field and gravity field on the fiber-reinforced generalized thermoelastic medium based on the 3PHL theory, CD theory and the G-N III theory. We obtain the following conclusions based on the above analysis:

1) It is clear that the hydrostatic initial stress, the temperature-dependent of thermal conductivity, the magnetic field and gravity play significant roles in all the physical quantities.

2) The phases lag τ_q and τ_θ have a great influence on the distribution of all physical quantities.

3) The curves in the context of the 3PHL theory, CD, theory and the G-N III theory, decrease exponentially with increasing z; this indicates that the thermoelastic waves are unattenuated and non-dispersive, while purely thermoelastic waves undergo both attenuation and dispersion.

4) The deformation of a generalized thermoelastic medium depends on the nature of the applied force as well as the type of boundary conditions.

5) Analytical solutions based upon the state-space approach analysis of the thermoelastic problem in solids have been developed and utilized.

6) There are significant differences in the field quantities under the G-N III theory, 3PHL model and CD theory due to the phase-lag of temperature gradient and the phase-lag of heat flux.

Funding

The author(s) received no financial support for the research, authorship, and/or publication of this article.

Acknowledgments

The research described in this paper was not financially supported by the Natural Science Foundation.

References

Abbas, I.A. (2014a), "Three-phase lag model on thermoelastic interaction in an unbounded fiber-reinforced anisotropic medium with a cylindrical cavity", *J. Comput. Theor. Nanosci*., **11**(4), 987-992. https://doi.org/10.1166/jctn.2014.3454

Abbas, I.A. (2014b), "Eigenvalue approach for an unbounded medium with a spherical cavity based upon two-temperature generalized thermoelastic theory", *J. Mech. Sci. Tech*., **28** (10), 4193-4198. https://doi.org/ 10.1007/s12206-014-0932-6

Abbas, I.A., Abd-alla, A.N. and Othman, M.I.A. (2011), "Generalized magneto-thermoelasticity in a fibre-reinforced anisotropic half-space", *Int. J. Thermophys.*, **32**(5), 1071-1085. https://doi.org/10.1007/s10765-011-0957-3

Abbas, I.A. and Othman, M.I.A. (2012), "Generalized thermo-elastic interaction in a fibre-reinforced anisotropic half-space under hydrostatic initial stress", *J. Vib. Control*, **18**(2), 175-182. https://doi.org/ 10.1177/1077546311402529

Abbas, I.A. and Youssef, H.M. (2013), "Two-temperature generalized thermoelasticity under ramp-type heating by finite element method", *Meccanica*, **48**(2), 331-339. https://doi.org/10.1007/s11012-012-9604-8

Ahmad, F. and Khan, A. (2001), "Effect of rotation on wave propagation in a transversely isotropic medium", *Math. Prob. Eng*., **7**(2), 147-154. http://dx.doi.org/10.1155/S1024123X01001582

Belfield, A.J., Rogers, T.G. and Spencer, A.J.M. (1983), "Stress in elastic plates reinforced by fibre lying in concentric circles", *J. Mech. Phys. Solids*, **31**, 25-54. https://doi.org/10.1016/0022-5096(83)90018-2.

England, A.H. and Rogers, T.G. (1973), "Plane crack problems for ideal fibre-reinforced materials", *Q. J. Mech. Appl. Math*., **26**, 303-320. https://doi.org/doi.org/10.1093/qjmam/26.3.303.

Green, A.E. and Lindsay, K.A. (1972), "Thermoelasticity", *J.*

Elast. **2**, 1–7. https://doi.org/10.1007/BF00045689.
Green, A.E. and Naghdi, P.M. (1991), "A re-examination of the basic postulate of thermo-mechanics", *Proc. Roy. Soc*., London. **432**, 171–194. https://doi.org/10.1098/rspa.1991.0012.
Green, A.E. and Naghdi, P.M. (1992), "On undamped heat waves in an elastic solid", *J. Therm. Stress.*, **15**, 253-264. https://doi.org/10.1080/01495739208946136.
Green, A.E. and Naghdi, P.M. (1993), "Thermoelasticity without energy dissipation", *J. Elast*. 31, 189–208. https://doi.org/10.1007/BF00044969.
Hetnarski, R.B. and Ignaczak, J. (1999), "Generalized thermo-elasticity", *J. Therm. Stress*, **22**, 451–476. https://doi.org/10.1080/014957399280832.
Lord, H.W. and Shulman Y. (1967), "A generalized dynamical theory of thermoelasticity", *J. Mech. Phys. Solid*, **15**, 299–309. https://doi.org/10.1016/0022-5096(67)90024-5
Marin, M., Baleanu, D. and Vlase, S. (2017), "Effect of Micro-temperatures for micropolar thermoelastic bodies", *Struct. Eng. Mech*., **61**(3), 381-387. https://doi.org/ https://doi.org/10.12989/sem.2017.61.3.381
Marin, M. and Craciun, E.M. (2017), "Uniqueness results for a boundary value problem in dipolar thermoelasticity to model composite materials", *Compos. Part B Eng.*, **126**, 27-37. https://doi.org/10.1016/j.compositesb.2017.05.063
Marin, M. and Florea, O. (2014), "On temporal behaviour of solutions in thermoelasticity of porous micro-polr bodies", *An. St. Univ. Ovidius Constanta*, **22**(1), 169-188. https://doi.org/ 10.2478/auom-2014-0014
Marin, M. and Nicaise, S. (2016), "Existence and stability results for thermoelastic dipolar bodies with double porosity", *Continuum Mech. Thermodynamics*, **28**(6), 1645-1657. https://doi.org/10.1007/s00161-016-0503-4
Montanaro, A. (1999), "On singular surface in isotropic linear thermoelasticity with initial stress", *J. Acoustical Society America*, **106**, 1586-1588. https://doi.org/ 10.1121/1.427154.
Noda, N. (1986), *Thermal Stresses in Materials with Temperature-Dependent Properties*, Thermal Stresses I, R.B. Hetnarski (Editor), North-Holland, Amsterdam.
Othman, M.I.A. and Abbas, I.A. (2011), "Effect of rotation on plane waves at the free surface of a fibre-reinforced thermoelastic half-space using the finite element method", *Meccanica*, **46**(2), 413-421. https://doi.org/10.1007/s11012-010-9322-z
Othman, M.I.A. and Abbas, I.A. (2012), "Generalized thermo-elasticity of thermal-shock problem in a non-homogeneous isotropic hollow cylinder with energy dissipation", *Int. J. Thermophys*., **33**(5), 913-923. https://doi.org/10.1007/s10765-012-1202-4
Othman, M.I.A. and Said, S.M. (2012), "The effect of mechanical force on generalized thermoelasticity in a fiber-reinforced under three theories", *Int. J. Thermophys.*, **33**(6), 1082-1099. https://doi.org/10.1007/s10765-012-1203-3
Othman, M.I.A., Abouelregal, A.E. and Said, S.M. (2019), "The effect of variabile thermal conductivity on an infinite fiber-reinforced thick plate under initial stress", *J. Mech. Materials Struct*., **14**(2), 277-293. https://doi.org/10.2140/jomms.2019.14.277.
Othman, M.I.A. and Said, S.M. (2014), "2-D problem of magneto-thermoelasticity fiber-reinforced medium under temperature-dependent properties with three-phase-lag theory", *Meccanica*, **49**(5), 1225-1243. https://doi.org/ 10.1007/s11012-014-9879-z
Othman, M.I.A. and Atwa, S.Y. (2014), "Effect of rotation on a fiber-reinforced thermoelastic under Green-Naghdi theory and influence of gravity", *Meccanica*, **49**(1), 23-36. https://doi.org/ 10.1007/s11012-013-9748-1
Othman, M.I.A. and Said, S.M. (2015), "The effect of rotation on a fibre-reinforced medium under generalized magneto-thermo-elasticity with internal heat source", *Mech. Adv. Materials Struct.*, **22**(3), 168-183. https://doi.org/ 10.1080/15376494.2012.725508
Othman, M.I.A., Sarkar, N. and Said, S.M. (2013), "Effect of hydrostatic initial stress and gravity field on a fiber-reinforced thermoelastic medium with fractional derivative heat transfer", *Multi. Model. Materials Struct*., 9(3), 410-426. https://doi.org/10.1108/MMMS-11-2012-0026
Pipkin, A.C. (1973), *In Finite Deformations of Ideal Fiber-Reinforced Composites*, Edited by G.P. Sendeckyi. Academic Press, New York.
Quintanilla, R. and Racke, R. (2008), "A note on stability in three-phase-lag heat conduction", *Int. J. Heat Mass Transfer,* **51**, 24–29.
Roy Choudhuri, S.K. (1984), "Electro-magneto-thermoelastic plane waves in rotating media with thermal relaxation", *Int. J. Eng. Sci*., **22**(5), 519-530. https://doi.org/10.1016/0020-7225(84)90054-5
Said, S.M. and Othman, M.I.A. (2016), "Wave Propagation in a two-temperature fiber-reinforced magneto-thermoelastic medium with three-phase-lag model", *Struct. Eng. Mech*., **57**(2), 201-220. http://dx.doi.org/10.12989/sem.2016.57.2.201
Zenkour, A.M. and Abbas, I.A. (2014), "A generalized thermo-elasticity problem of an annular cylinder with temperature-dependent density and material properties", *Int. J. Mech. Sci*., **84**, 54-60. https://doi.org/10.1016/j.ijmecsci.2014.03.016
Zorammuana, C. and Singh, S.S. (2015), "SH-wave at a plane interface between homogeneous and inhomogeneous fibre-reinforced elastic half-spaces", *Ind. J. Materials Sci*., **2015**, 1-8. http://dx.doi.org/10.1155/2015/532939

CC